Journal of Orthopaedic Surgery and Research

RESEARCH

Open Access

Abnormal patellar sagittal spatial kinematics in patients with patellofemoral pain: an in vivo dynamic CT study

Mao Yuan[1†], Yurou Chen[2†], Jia Li[1], Haitao Yang[1], Fan Yu[1*] and Furong Lv[1*]

Abstract

Background Patellofemoral joint kinematics is a complex three-dimensional(3D) motion, involving shift and rotation in the coronal, sagittal, and axial directions. Quantifying patellar tracking only at the axial level of the patella or with two-dimensional(2D) parameters may not be comprehensive. The current study sought to explore the spatial kinematics characteristics of the patella in three directions, especially the sagittal plane in patients with patellofemoral pain (PFP) based on Four-dimensional computed tomography (4D-CT).

Methods A total of 35 knees with PFP and 35 controls from March 2023 to May 2024 were evaluated. 3D shift and tilt of the patella were measured in the patellofemoral joint coordinate system established by MIMICS. The 3D shift and tilt of the patella in three directions (coronal, sagittal, and axial) were evaluated. Differences between groups were analyzed using two-way repeated measures ANOVA.

Results The 3D $tilt_{sagittal}$ and 3D $tilt_{axial}$ trends differed between the two groups ($P=0.020$, 0.018, respectively). The 3D $shift_{sagittal}$ at knee flexions of 50° to 70° was significantly increased in the PFP group compared to the control group ($P=0.009$, 0.015, respectively). The 3D $tilt_{sagittal}$ was significantly greater in the PFP group than in the control group at -10° to 10° and 50° to 70° of knee flexion ($P=0.004$, 0.005, 0.046, 0.007, respectively). The 3D $tilt_{axial}$ was significantly greater in the PFP group than in the control group at -10° to 0° and 40° to 70° of knee flexion ($P=0.033$, 0.011, 0.004, 0.015, respectively). The 3D $shift_{coronal}$ at knee flexions of -10° to 20° were significantly decreased in the PFP group compared to the control group ($P=0.002$, <0.001, 0.018, respectively).

Conclusion It is necessary to evaluate the spatial position characteristics of the patellofemoral joint and the stability of the patella from multiple planes and angles at the dynamic level. Analyzing the spatial multi-plane kinematic characteristics of the patellofemoral joint may help in determining the etiology of PFP.

Keywords Patellofemoral pain, Four-dimensional computed tomography, Kinematics, Shift, Tilt

†Mao Yuan and Yurou Chen contributed equally to this work. Fan Yu and Furong Lv are co-corresponding authors.

*Correspondence:
Fan Yu
2836373598@qq.com

Furong Lv
lfr918@sina.com
[1]Department of Radiology, The First Affiliated Hospital of Chongqing Medical University, No.1 Youyi Road, Yuzhong District, Chongqing 400000, PR China
[2]Department of Oncology, The First Affiliated Hospital of Chongqing Medical University, Chongqing, China

Introduction

Patellofemoral pain (PFP) is one of the most common knee disorders, especially prevalent in adolescents and physically active adults [1–4]. Long-lasting PFP may be associated with the development of patellofemoral osteoarthritis [5–7]. With a high incidence of PFP and a poor prognosis, early detection and prevention are necessary [8, 9]. Clinical examination is the basis for the diagnosis of PFP, but because the etiology of PFP is multifactorial, there is a wide variety of approaches to clinical assessment, and no consensus has been reached on the diagnosis of PFP [10]. The clinical evaluation methods of PFP mainly include patellar palpation, patellofemoral compression test, and pain during squatting [11, 12]. However, many patients with PFP may have reduced knee motion due to pain, so this diagnostic approach may only identify patients with higher levels of pain or who are still actively exercising [13]. Reduced effective knee motion may lead to reduced muscle function around the knee and thus reduced patellofemoral joint stability [14], which in turn is detrimental to the long-term outcome of PFP therapy. Some studies have proposed patellar maltracking/malalignment as the cause of PFP [15, 16]. The "J" sign is one of the most common physical examination techniques used in clinical practice to diagnose patellar maltracking, but the visual assessment of patellar tracking varies greatly among different orthopedic surgeons, resulting in inconsistent judgments on patellofemoral stability [17], which emphasizes the importance of objective quantification of patellar tracking [18].

Normal patellofemoral joint motion is maintained by a dynamic balance between the skeletal structure and the surrounding soft tissues [19]. Four-dimensional computed tomography (4D-CT), also known as dynamic CT, is an effective examination that can combine skeletal anatomy with the functional status of movement, providing objective functional data for the assessment of patellofemoral stability [20, 21]. Miho J. Tanaka et al. [22] used 4D-CT to objectively quantify patellar maltracking patterns. The patellar axial motion pattern (J-sign) was complemented by their study, patients with a J-sign severity greater than grade 2 may have symptoms of patellar instability. Ariel. A. Williams et al. [23] found that in patients with unilateral patellofemoral instability, tibial tubercle-trochlear groove distance, lateral patellar tilt, and bisect offset were significantly higher on the affected side than on the healthy side. However, these 4D-CT-based studies have mainly explored changes in the axial position of the patella, ignoring shift and tilt changes of the patella in other planes, especially the sagittal plane. A study by Wilson NA et al. [24] found poor rotational alignment of the patella in the sagittal plane in patients with PFP. Given that patellar motion involves shift and rotation in the coronal, sagittal, and axial directions [25], quantifying patellar tracking only at the axial level of the patella may not be comprehensive.

Patellar tracking is a complex three-dimensional movement and the use of two-dimensional linear parameters to assess the three-dimensional positional relationship between the patella and femur may be inaccurate [26]. A growing body of research proposes to focus on three-dimensional measurements [27, 28]. Yet, an extensive search of the literature revealed no studies on three-dimensional measurement parameters to assess sagittal plane motion characteristics of the patella in patients with PFP. This study aimed to quantify the three-dimensional motion characteristics of the patella in three directions, especially the sagittal plane in patients with PFP based on 4D-CT. We hypothesized that there were abnormal movement patterns in 3D shift and tilt of the patella, and the occurrence of PFP may be related to abnormal movement of the patella in multiple planes and multiple angles.

Methods

Participants

Patients with PFP were recruited in an outpatient clinic from March 2023 to May 2024. Two orthopaedic surgeons with more than 6 years of clinical experience performed physical examination and clinical diagnosis of these patients. The inclusion criteria were as follows: (1) typical clinical signs and symptoms of PFP in the knee (typically presented as diffuse pain behind or around the patella), if both knees were symptomatic, both knees of one patient were included; (2) persistence of symptoms of PFP symptoms in the knee for at least 6 months; (3) Age between 16 and 45 years. The exclusion criteria were as follows: (1) a history of patellar dislocation or those with traumatic PFP onset; (2) a history of knee surgery; (3) ligamentous or meniscal injuries confirmed by magnetic resonance imaging; (4) femorotibial osteoarthritis and/or patellofemoral osteoarthritis[≥ Kellgren-Lawrence(KL) 3grade]; (5) The image is incomplete or of poor quality; and (6) contraindications to CT scan.

We recruited patients who required CT scanning for acute trauma or benign tumors of the contralateral leg, without signs of patellofemoral symptoms and no positive findings on physical examination or MRI. The control knees were the asymptomatic knees of this group of patients without PFP. The exclusion criteria were consistent with the patient group. This case-control study was approved by our Institutional Review Board (No. 2023 – 360). Informed consent was obtained from all patients.

4D- CT protocol

4D-CT scanning was performed on a wide detector CT scanner equipped with 320 0.5-mm detectors (Aquilion

ONE, Canon Medical Systems, Otawara, Japan) in dynamic CT continuous scan mode without table feed. The participant was positioned supine with the thighs secured to the table using a strap, while the calves were placed outside the gantry without restraint, allowing the knees to flex and extend freely (Fig. 1). During the 10-second scan, the participant performed approximately 1.5 cycles of knee motion (flexion-extension-flexion) at a constant speed, ranging from – 10° hyperextension to 70° flexion. The scan protocol included a slice thickness of 0.5 mm, slice spacing of 0.5 mm, tube rotation of 0.35 s, tube output of 100 kV and 70 mA, a time interval of 0.5 s, and a DFOV of 500 × 500 × 160 mm. A total of 21 frame images were obtained. During the scan, a lead protector covered each participant from the neck to the proximal thigh to minimize ionizing radiation exposure. The study by TanakaMJ et al. [22] clearly stated the radiation dose for 4D-CT examination of the knee joint: when the same amount of image information is obtained, the effective dose of a 64-slice CT machine is more than three times that of a 320-slice CT scanner.

Patellofemoral joint kinematic coordinate system

Mimics 21.0 and 3-matic 13.0 (Materialize, Leuven, Belgium) software were used in this study. DICOM data were imported into Mimics 21.0 to segment and reconstruct 3D models of the patella and femur. The spatial relationship between the patella and femur was preserved. Anatomical location points were selected on the 3D skeletal model and a coordinate system was created (Fig. 2A-B). The coordinate system of the patellofemoral joint was used to describe the spatial motion of the patella relative to the femur (Fig. 2C). The patellar reference point was the calculated center of gravity of the patella by the software. The patellar ridge proximal point (PRPP) was defined as the most proximal point on the patellar ridge. The patella distal pole (PDP) was defined as the most distal point of the patella. The long axis of the patella was defined as the line between PRPP and PDP. PMP (patella medial pole) was defined as the most medial point of the patella. PLP (patella lateral pole) was defined as the most lateral point of the patella. The short axis of the patella was defined as the line between PMP and PLP. The lateral femoral condyle point (LFC) was defined as the most prominent point of the lateral femoral condyle. The medial femoral condyle point (MFC) was defined as the most prominent point of the medial femoral condyle. The origin of the coordinate system was defined as the midpoint of the line connecting LFC and MFC. Roman arch (RA) was defined as the most concave point of a Roman arch. The *X0Y* plane was established by the LFC, MFC, and RA points, and the *X0Y* plane was perpendicular to the long axis of the femur. A normal vector perpendicular to the *X0Y* plane was created based on the origin. The *X0Z* plane was created based on the LFC, MFC, and an arbitrary point on the normal vector (Fig. 2C).

Measurement of parameters

We used 3D shift (including 3D $\text{shift}_{\text{sagittal}}$, 3D $\text{shift}_{\text{axial}}$, and 3D $\text{shift}_{\text{coronal}}$) and 3D tilt (including 3D $\text{tilt}_{\text{sagittal}}$, 3D $\text{tilt}_{\text{axial}}$, and 3D $\text{tilt}_{\text{coronal}}$) to describe the relative motion between the patella and femur in three directions: sagittal, axial, and coronal. The 3D parameters were measured using 3-matic 13.0. 3D $\text{shift}_{\text{sagittal}}$ was defined as the spatial distance in the *Z*-axis direction between the patellar reference point and the origin (Fig. 3a). The patellar reference point moved upward relative to the *X0Y* plane to be positive. 3D $\text{shift}_{\text{axial}}$ was defined as the spatial distance in the *X*-axis direction between the patellar reference point and the origin (Fig. 3b). The patellar reference point moved outward relative to the *Z*-axis to be positive. 3D $\text{shift}_{\text{coronal}}$ was defined as the spatial distance in the *Y*-axis direction between the patellar reference point and the origin (Fig. 3c). The patellar reference point moved

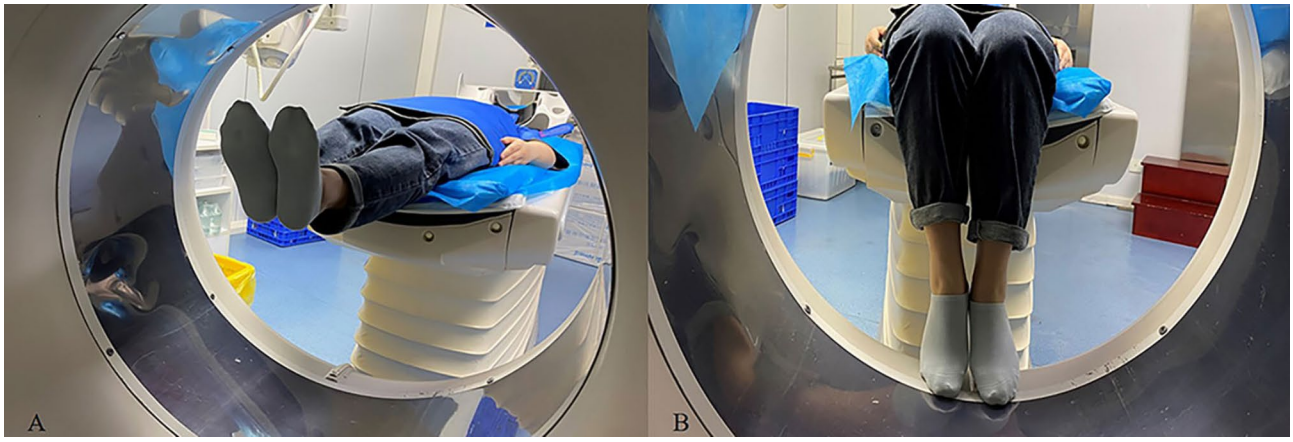

Fig. 1 Position of the subject during 4D-CT scan. The subject is in a supine position and the subject is asked to fully extend and flex both legs in approximately 10 s

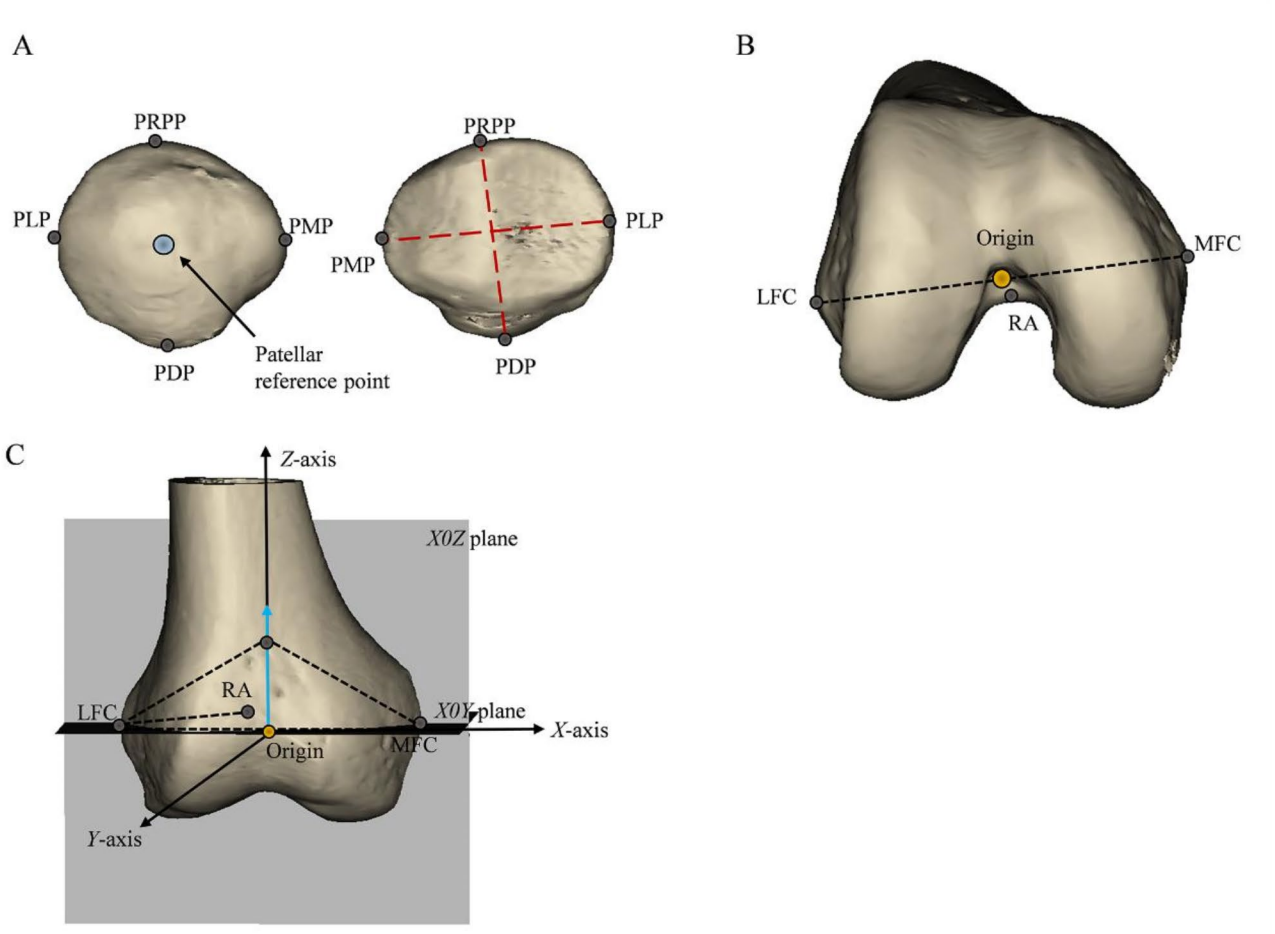

Fig. 2 3D knee joint model with bone landmarks and establishment of patellofemoral joint coordinate system. (**A**) Patella anatomical landmarks. Patellar reference point: center of gravity of the patella; PRPP: patellar ridge proxima point; PDP: patella distal pole; Long axis of the patella: the line between PRPP and PDP. PMP, patella medial pole. PLP, patella lateral pole. The short axis of the patella: the line between PMP and PLP. (**B**) Femur anatomical landmarks. LFC: lateral femoral condyle; MFC: medial femoral condyle point; Origin: the midpoint of the line connecting LFC and MFC; RA: Roman arch. (**C**) Establishment of patellofemoral joint coordinate system. The *X0Y* plane was established by the LFC, MFC, and RA points. A normal vector perpendicular to the *X0Y* plane was created based on the origin. The *X0Z* plane was created based on the LFC, MFC, and an arbitrary point on the normal vector

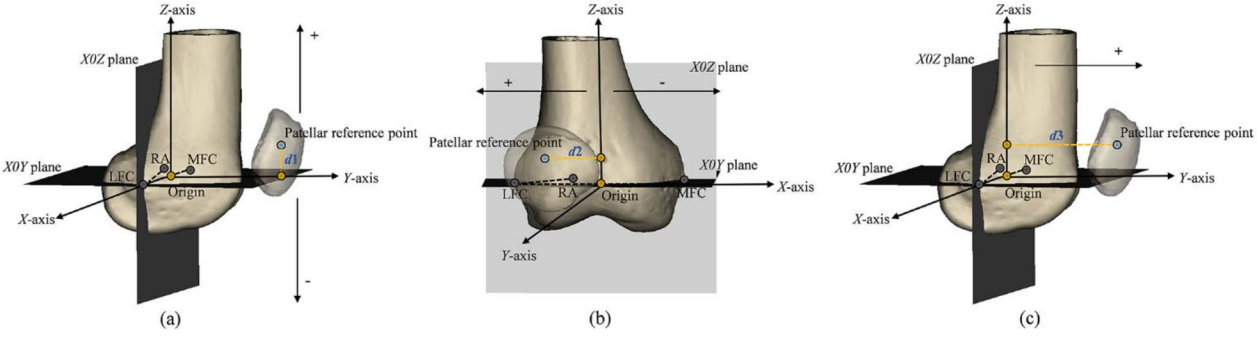

Fig. 3 3D shift measurements. (**a**): 3D $shift_{sagittal}$ was represented as d1, which was the spatial distance in the *Z*-axis direction between the patellar reference point and the origin. The patellar reference point moved upward relative to the *X0Y* plane to be positive. (**b**): 3D $shift_{axial}$ was represented as d2, which was the spatial distance in the *X*-axis direction between the patellar reference point and the origin. The patellar reference point moved outward relative to the *Z*-axis to be positive. (**c**): 3D $shift_{coronal}$ was represented as d3, which was the spatial distance in the *Y*-axis direction between the patellar reference point and the origin. The patellar reference point moved forward relative to the *X0Z* plane to be positive

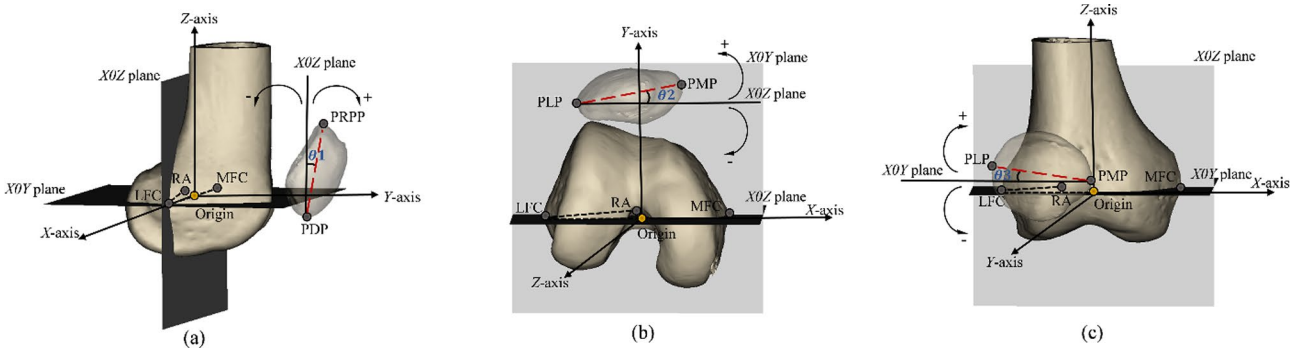

Fig. 4 3D tilt measurements. (**a**): 3D $tilt_{sagittal}$ was represented as θ 1, which was the spatial angle between the long axis of the patella and the *X0Z* plane. The angle was positive when the long axis of the patella was tilted forward relative to the *X0Z* plane. (**b**): 3D $tilt_{axial}$ was represented as θ 2, which was the spatial angle between the short axis of the patella and the *X0Z* plane. The angle was positive when the short axis of the patella was tilted outward relative to the *X0Z* plane. (**c**): 3D $tilt_{coronal}$ was represented as θ 3, which was the spatial angle between the short axis of the patella and the *X0Y* plane. The angle was positive when the short axis of the patella was tilted upward relative to the *X0Y* plane

Fig. 5 Method for measuring the flexion angle of the knee. (**A**) - (**B**) represents measurements of knee flexion angles in images from different time frames using the same measurement method. Two circles are made at the level of the median of the tibia and femur respectively. The edges of the circles intersect the cortex of the anterior and posterior margins of the bone and the center of the other circle. The long axes of the tibia and femur are the lines joining the centers of the two circles. The angle between the long axes of the tibia and femur is the knee flexion angle. (**A**) Angle measurements with the subject in the extended position; (**B**) knee flexed at 60°

forward relative to the *X0Z* plane to be positive. 3D $shift_{sagittal}$, 3D $shift_{axial}$, and 3D $shift_{coronal}$ were normalized to the transepicondylar axis (TEA) and expressed as a percentage of the TEA.

3D $tilt_{sagittal}$ was defined as the spatial angle between the long axis of the patella and the *X0Z* plane (Fig. 4a). The angle was positive when the long axis of the patella was tilted forward relative to the *X0Z* plane. 3D $tilt_{axial}$ was defined as the spatial angle between the short axis of the patella and the *X0Z* plane (Fig. 4b). The angle was positive when the short axis of the patella was tilted outward relative to the *X0Z* plane. 3D $tilt_{coronal}$ was defined as the spatial angle between the short axis of the patella and the *X0Y* plane (Fig. 4c). The angle was positive when the short axis of the patella was tilted upward relative to the *X0Y* plane.

In this study, a total of 21 consecutive images (knee flexion −10° to 70°) were obtained for each scan, and measurements were performed on each image. To observe more or less movement of the patella within the PFP or control group, we normalized the data to the extended position. The knee flexion angle was defined as the angle between the long axis of the femur and the long axis of the tibia (Fig. 5). Two musculoskeletal radiologists

Table 1 Participant characteristics

Characteristic	PFP group (*n* = 35)	Control group (*n* = 35)	*P* value
Gender (males/females)	3/18	22/13	0.001
Side (left/right)	19/16	15/20	0.339
Age, y	32.62 ± 7.73	31.29 ± 8.16	0.549
Age range, y	16–45	17–44	NA
BMI (body mass index), kg/m^2	21.87 ± 2.34	22.44 ± 3.40	0.507
Insall-Salvati index	1.03 ± 0.11	1.00 ± 0.11	0.244
VAS pain scores (out of 10)			
Pain during a typical day	2.10 ± 0.70	—	NA
Pain during a provocative activity	4.19 ± 1.08	—	NA

with more than 5 years of clinical experience performed the measurements independently after the data from both groups had been blinded and randomly distributed. To assess intra-observer reliability, one of the radiologists repeated all measurements after a minimum interval of 4 weeks.

Statistical tests

Statistical analyses were performed using SPSS software (version 17.0; SPSS, Chicago, IL, USA), with a significance level set at 0.05. In demographic data, count data were compared between two groups using the chi-square test. The Shapiro-Wilk test was used for normality testing. Continuous variables with a normal distribution were expressed as mean ± standard deviations and were analyzed using two-way repeated measures analysis of variance (ANOVA). A Greenhouse-Geisser correction was applied if the analysis failed a Mauchly test for sphericity. Intraclass correlation coefficients (ICCs) was used to assess the inter- and intraobserver reliability measurements for two parameters.

The sample size was calculated a priori with G*Power (version 3.1.9.7) based on a 5% probability of deviating norm values in a population, considering a 95% confidence interval (CI). With an alpha of 0.05 and a statistical power of 0.95, a sample size of at least 12 knees per group, totaling 24 knees, was required to obtain reliable results.

Results

Demographic characteristics of subjects in the two groups

During the study period, 42 knees with PFP underwent 4D-CT scans, 5 knees were excluded due to insufficient knee flexion angle, 2 knees were excluded due to patellofemoral osteoarthritis (≥ KL grade 3) and a total of 35 knees (19 left, 16 right) of 21 patients (3 males and 18 females, age range 16–45 years, mean age 32.62 ± 7.73 years) were finally included in the PFP group. All patients included in the PFP group had bilateral PFP. In the control group, 40 participants completed 4D-CT scans, 2 knees were excluded due to heavy image motion artifacts, and 3 knees were excluded due to insufficient knee flexion angle. Finally, there were 35 knees (15 left, 20 right) of 35 participants(22 males and 13 females, age range 17–44 years, mean age 31.29 ± 8.16 years) in the control group. There was a significant difference in sex between the two groups of subjects ($P = 0.001$), but no significant differences in age, side, and body mass index. In this study, patients with PFP primarily exhibited mild to moderate pain in the patellofemoral joint (Table 1).

Table 2 Consistency analysis of intra-and interobserver parameter measurements

3D parameters	Intraobserver reliability(95%CI)	Interobserver reliability(95%CI)
3D $shift_{sagittal}$	0.996(0.992,0.998)	0.987(0.977,0.993)
3D $tilt_{sagittal}$	0.992(0.987,0.995)	0.983(0.973,0.989)
3D $shift_{axial}$	0.980(0.967,0.988)	0.949(0.624,0.983)
3D $tilt_{axial}$	0.997(0.995,0.998)	0.991(0.937,0.997)
3D $shift_{coronal}$	0.987(0.816,0.996)	0.960(0.807,0.984)
3D $tilt_{coronal}$	0.991(0.987,0.994)	0.978(0.899,0.991)

Intra-and interobserver reliability of the parameter measurements

The intraclass correlation coefficients (ICCs) for intraobserver reliability of 3D shift (including 3D $shift_{sagittal}$, 3D $shift_{axial}$, and 3D $shift_{coronal}$) and 3D tilt (including 3D $tilt_{sagittal}$, 3D $tilt_{axial}$, and 3D $tilt_{coronal}$) measurements ranged from 0.980 to 0.997, while interobserver reliability ranged from 0.949 to 0.991 (Table 2), indicating good reliability both within and between observers.

Comparison of 3D shift and tilt between the PFP group and the control group

The trends of 3D $shift_{sagittal}$, 3D $shift_{sagittal}$ normalized to the TEA, and 3D $shift_{sagittal}$ normalized to the full extension were consistent between the two groups ($P = 0.244$, 0.698, 0.962, respectively). The trends of 3D $shift_{axial}$, 3D $shift_{axial}$ normalized to the TEA, and 3D $shift_{axial}$ normalized to the full extension were consistent between the two groups ($P = 0.986$, 0.637, 0.590, respectively). The trends of 3D $shift_{coronal}$ and 3D $shift_{coronal}$ normalized to the full extension were consistent between the two groups ($P = 0.053$, 0.903, respectively). The trends of 3D $shift_{coronal}$ normalized to the TEA were different between the two groups ($P = 0.003$). (Fig. 6)

The trends of 3D $tilt_{sagittal}$ were different between the two groups ($P = 0.020$). The trends of 3D $tilt_{sagittal}$ normalized to the full extension were consistent between the two groups ($P = 0.285$). The trends of 3D $tilt_{axial}$ were different between the two groups ($P = 0.018$). The trends of 3D $tilt_{axial}$ normalized to the full extension were consistent between the two groups ($P = 0.448$). The trends of 3D $tilt_{coronal}$ and 3D $tilt_{coronal}$ normalized to the full extension

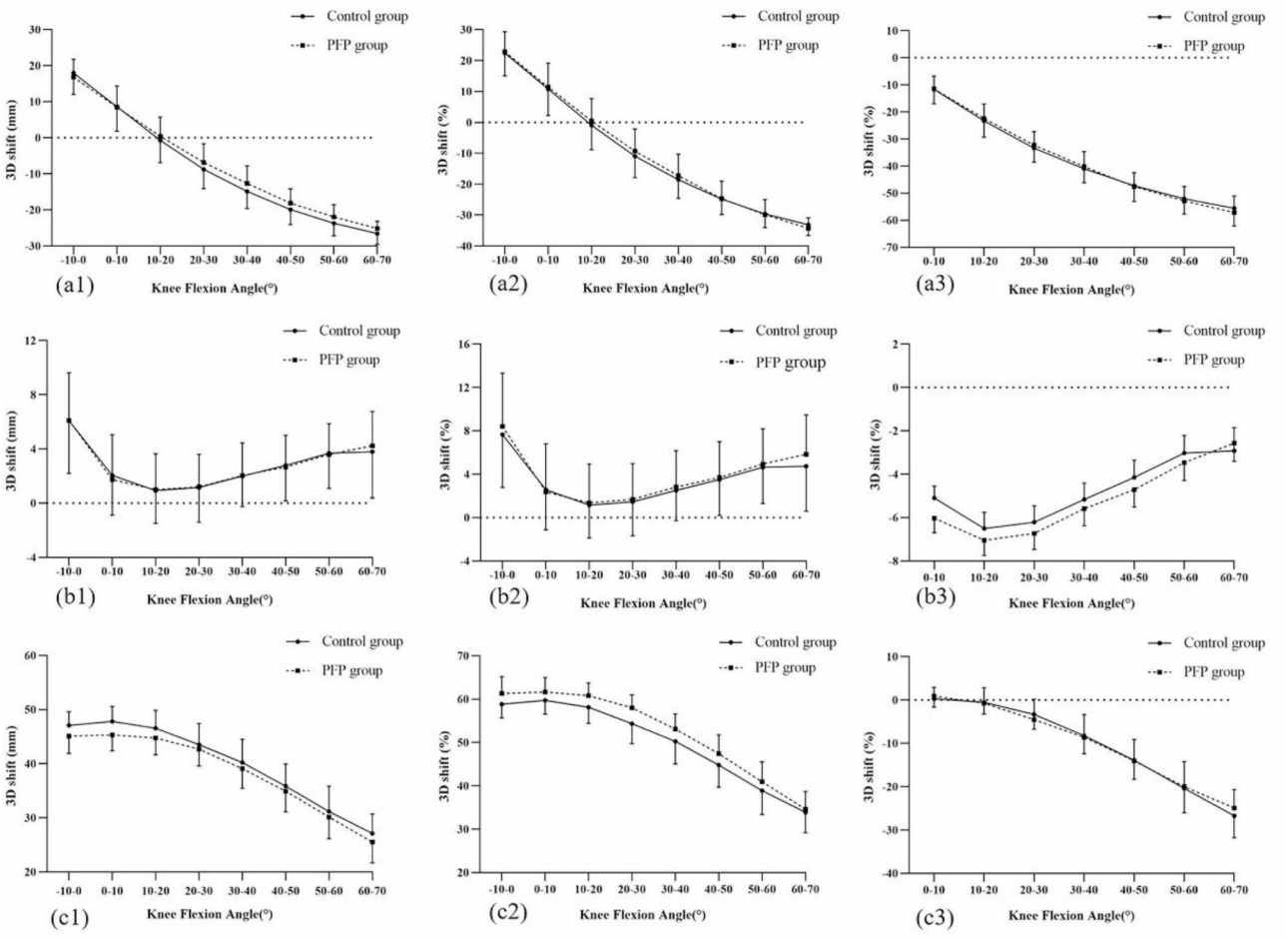

Fig. 6 Curve of mean (± standard deviation) interpolated data of the 3D shift. (**a** 1-3): 3D shift of the sagittal plane; (**b** 1-3): 3D shift of the axial plane; (**c** 1-3): 3D shift of the coronal plane; (**a** 2-c2): 3D shift was normalized to the transepicondylar axis (TEA) and expressed as a percentage of the TEA; (**a** 3-c3): 3D shift was normalized to the full extension. The trends of 3D $shift_{sagittal}$, 3D $shift_{sagittal}$ normalized to the TEA, and 3D $shift_{sagittal}$ normalized to the full extension were consistent between the two groups ($P = 0.244$, $P = 0.698$, $P = 0.962$, respectively). The trends of 3D $shift_{axial}$, 3D $shift_{axial}$ normalized to the TEA, and 3D $shift_{axial}$ normalized to the full extension were consistent between the two groups ($P = 0.986$, $P = 0.637$, $P = 0.590$, respectively). The trends of 3D $shift_{coronal}$ and 3D $shift_{coronal}$ normalized to the full extension were consistent between the two groups ($P = 0.053$, $P = 0.903$, respectively). The trends of 3D $shift_{coronal}$ normalized to the TEA were different between the two groups ($P = 0.003$)

were consistent between the two groups ($P = 0.628$, 0.669, respectively) (Fig. 7).

The differences between the two groups at the same knee flexion angles were compared. As shown in Table 3, the 3D $shift_{sagittal}$ at knee flexions of 50° to 70° were significantly increased in the PFP group compared to the control group ($P = 0.009$, 0.015, respectively). There were no significant differences between the two groups in the 3D $shift_{sagittal}$ normalized to the TEA and 3D $shift_{sagittal}$ normalized to the full extension at -10° to 70° of knee flexions (all $P > 0.05$). There were no significant differences between the two groups in the 3D $shift_{axial}$, 3D $shift_{axial}$ normalized to the TEA, and 3D $shift_{axial}$ normalized to the full extension at -10° to 70° of knee flexions (all $P > 0.05$). The 3D $shift_{coronal}$ at knee flexions of -10° to 20° were significantly decreased in the PFP group compared to the control group ($P = 0.002$, < 0.001, 0.018, respectively). The 3D $shift_{coronal}$ normalized to the TEA at knee flexions of -10° to 50° were significantly increased in the PFP group compared to the control group ($P = 0.002$, 0.007, 0.001, < 0.001, 0.012, 0.024, respectively). There were no significant differences between the two groups in the 3D $shift_{coronal}$ normalized to the full extension at -10° to 70° of knee flexions (all $P > 0.05$).

As shown in Table 4, the 3D $tilt_{sagittal}$ was significantly greater in the PFP group than in the control group at -10° to 10° and 50° to 70° of knee flexion ($P = 0.004$, 0.005, 0.046, 0.007, respectively). There were no significant differences between the two groups in the 3D $tilt_{sagittal}$ normalized to the full extension at -10° to 70° of knee flexions (all $P > 0.05$). The 3D $tilt_{axial}$ was significantly greater in the PFP group than in the control group at -10° to 0° and 40° to 70° of knee flexion ($P = 0.033$, 0.011, 0.004, 0.015, respectively). There were no significant differences

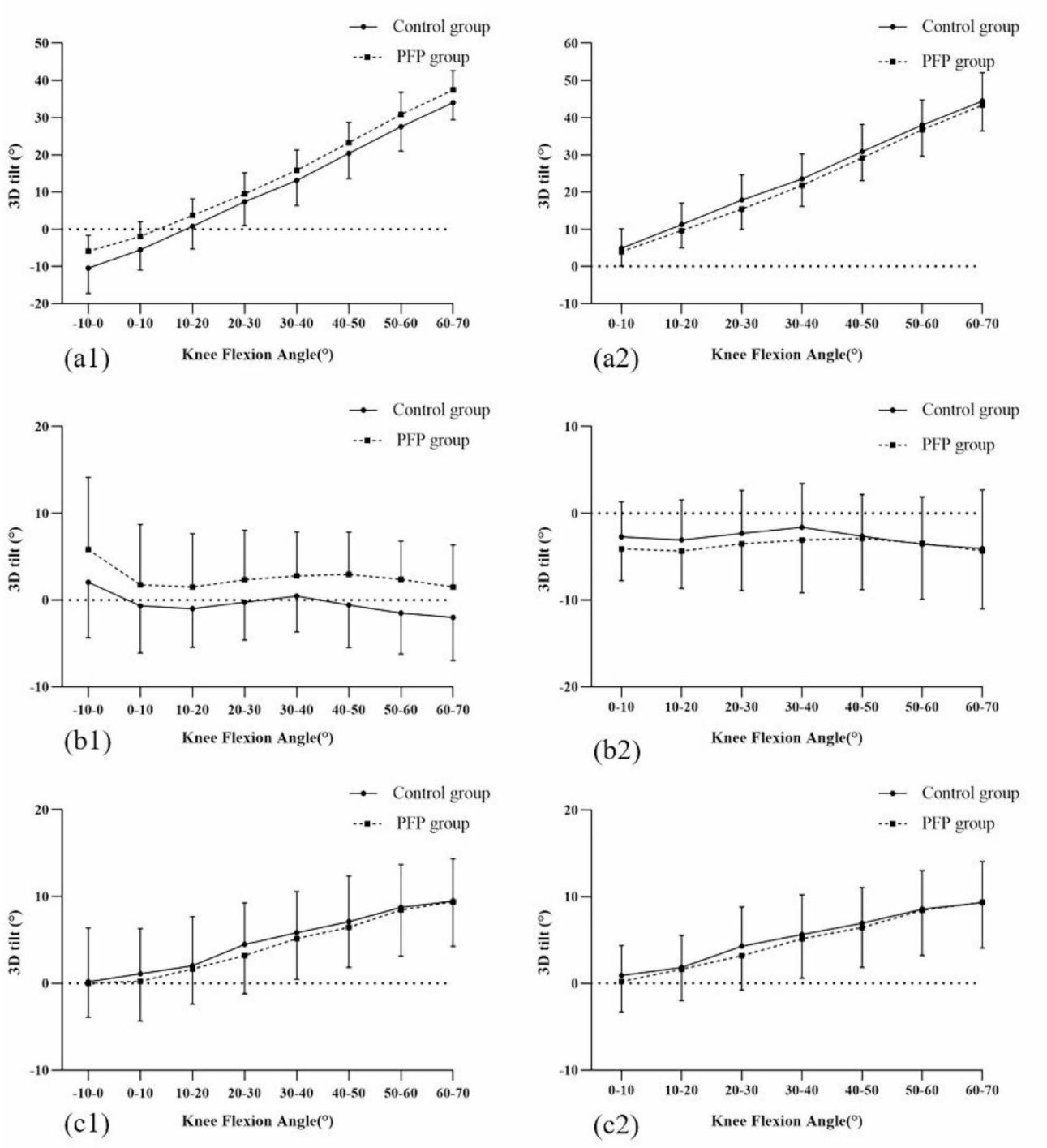

Fig. 7 Curve of mean (± standard deviation) interpolated data of the 3D tilt. (**a** 1-2): 3D tilt of the sagittal plane; (**b** 1-2): 3D tilt of the axial plane; (**c** 1-2): 3D tilt of the coronal plane; (**a** 2-c2): 3D tilt was normalized to the full extension. The trends of 3D $tilt_{sagittal}$ were different between the two groups ($P = 0.020$). The trends of 3D $tilt_{sagittal}$ normalized to the full extension were consistent between the two groups ($P = 0.285$). The trends of 3D $tilt_{axial}$ were different between the two groups ($P = 0.018$). The trends of 3D $tilt_{axial}$ normalized to the full extension were consistent between the two groups ($P = 0.448$). The trends of 3D $tilt_{coronal}$ and 3D $tilt_{coronal}$ normalized to the full extension were consistent between the two groups ($P = 0.628$, $P = 0.669$, respectively)

Table 3 Comparison of the 3D shift parameter between the PFP group and control group

Flexion angle (°)	Sagittal			Axial			Coronal		
	PFP group	Control group	*P*-value	PFP group	Control group	*P*-value	PFP group	Control group	*P*-value
-10-0	16.83 ± 4.95	17.96 ± 5.95	0.357	6.10 ± 3.52	6.08 ± 3.89	0.975	45.10 ± 3.22	47.08 ± 2.53	**0.002**
	22.86 ± 6.49*	22.39 ± 7.34*	0.757*	8.41 ± 4.92*	7.66 ± 4.89*	0.461*	61.33 ± 3.86*	58.86 ± 3.19*	**0.002***
0–10	8.50 ± 5.89	8.62 ± 6.78	0.934	1.74 ± 3.31	2.05 ± 2.95	0.688	45.33 ± 2.93	47.80 ± 2.77	**<0.001**
	11.40 ± 7.78*	10.76 ± 8.58*	0.732*	2.38 ± 4.44*	2.57 ± 3.70*	0.852*	61.64 ± 3.34*	59.74 ± 3.19*	**0.007***
	-11.46 ± 4.72#	-11.63 ± 5.33#	0.890#	-6.03 ± 3.93#	-5.10 ± 3.23#	0.230#	0.32 ± 1.96#	0.88 ± 2.07#	0.256#
10–20	0.42 ± 5.31	-0.73 ± 6.18	0.423	0.99 ± 2.66	0.93 ± 2.41	0.930	44.75 ± 3.08	46.54 ± 3.29	**0.018**
	0.43 ± 7.25*	-0.92 ± 7.94*	0.482*	1.36 ± 3.58*	1.16 ± 3.03*	0.829*	60.82 ± 2.92*	58.15 ± 3.73*	**0.001***
	-22.43 ± 5.39#	-23.31 ± 5.98#	0.520#	-7.05 ± 4.10#	-6.50 ± 4.41#	0.527#	-0.51 ± 2.72#	-0.71 ± 3.58#	0.800#
20–30	-6.85 ± 5.21	-8.80 ± 5.31	0.165	1.20 ± 2.41	1.16 ± 2.56	0.938	42.68 ± 3.11	43.51 ± 3.90	0.348
	-9.37 ± 7.26*	-11.00 ± 6.89*	0.392*	1.68 ± 3.32*	1.45 ± 3.13*	0.781*	58.01 ± 2.98*	54.36 ± 4.64*	**<0.001***
	-32.23 ± 4.98#	-33.40 ± 5.14#	0.342#	-6.73 ± 4.40#	-6.21 ± 4.47#	0.524#	-3.32 ± 3.42#	-4.50 ± 4.70#	0.269#
30–40	-12.65 ± 4.85	-14.85 ± 4.77	0.083	2.04 ± 2.41	2.0 ± 2.24	0.949	39.10 ± 3.64	40.22 ± 4.27	0.250
	-17.30 ± 6.96*	-18.57 ± 6.03*	0.461*	2.82 ± 3.35*	2.50 ± 2.80*	0.692*	53.09 ± 3.51*	50.26 ± 5.20*	**0.012***
	-40.16 ± 5.51#	-40.96 ± 5.12#	0.487#	-5.59 ± 4.70#	-5.16 ± 4.44#	0.622#	-8.23 ± 4.17#	-8.60 ± 5.25#	0.768#
40–50	-18.11 ± 3.92	-19.94 ± 4.14	0.065	2.66 ± 2.35	2.79 ± 2.62	0.846	34.92 ± 3.80	35.84 ± 4.09	0.356
	-24.69 ± 5.65*	-24.87 ± 5.03*	0.894*	3.69 ± 3.32*	3.51 ± 3.33*	0.834*	47.44 ± 4.34*	44.79 ± 5.10*	**0.024***
	-47.55 ± 5.11#	-47.26 ± 5.78#	0.823#	-4.71 ± 4.72#	-4.15 ± 4.76#	0.538#	-13.89 ± 4.41#	-14.07 ± 4.99#	0.883#
50–60	-21.97 ± 3.40	-23.73 ± 3.51	**0.009**	3.59 ± 2.27	3.69 ± 2.60	0.878	30.17 ± 4.01	31.15 ± 4.69	0.351
	-29.95 ± 4.99*	-29.67 ± 4.44*	0.765*	4.95 ± 3.24*	4.64 ± 3.33*	0.720*	40.95 ± 4.63*	38.88 ± 5.49*	0.079*
	-52.81 ± 5.27#	-52.06 ± 5.62#	0.532#	-3.46 ± 4.89#	-3.02 ± 4.80#	0.646#	-20.38 ± 5.63#	-19.99 ± 5.79#	0.775#
60–70	-25.17 ± 2.01	-26.55 ± 3.04	**0.015**	4.24 ± 2.53	3.80 ± 3.42	0.548	25.53 ± 3.86	27.11 ± 3.62	0.100
	-34.31 ± 3.38*	-33.15 ± 3.49*	0.122*	5.84 ± 3.64*	4.74 ± 4.16*	0.244*	34.60 ± 4.09*	33.92 ± 4.71*	0.515*
	-57.17 ± 6.16#	-55.54 ± 6.53#	0.287#	-2.56 ± 4.95#	-2.92 ± 6.30#	0.762#	-26.73 ± 5.03#	-24.95 ± 4.27#	0.110#

*3D shift was normalized to the transepicondylar axis (TEA) and expressed as a percentage of the TEA

#3D shift was normalized to a set position (i.e. full extension)

Table 4 Comparison of the 3D tilt parameter between the PFP group and control group

Flexion angle (°)	Sagittal			Axial			Coronal		
	PFP group	Control group	*P*-value	PFP group	Control group	*P*-value	PFP group	Control group	*P*-value
-10-0	-5.91 ± 4.25	-10.45 ± 6.78	**0.004**	5.85 ± 8.29	2.07 ± 6.40	**0.033**	0.0243 ± 3.94	0.19 ± 6.19	0.910
0–10	-1.96 ± 3.90	-5.52 ± 5.45	**0.005**	1.75 ± 6.95	-0.65 ± 5.45	0.140	0.24 ± 4.58	1.11 ± 5.20	0.506
	3.95 ± 3.90#	4.93 ± 5.17#	0.374#	-4.10 ± 3.66#	-2.71 ± 4.04#	0.093#	0.22 ± 3.54#	0.92 ± 3.43#	0.426#
10–20	3.70 ± 4.45	0.81 ± 6.13	0.063	1.51 ± 6.12	-0.99 ± 4.45	0.071	1.66 ± 4.06	2.03 ± 5.65	0.779
	9.62 ± 4.68#	11.26 ± 5.75#	0.234#	-4.34 ± 4.33#	-3.06 ± 4.62#	0.188#	1.63 ± 3.63#	1.84 ± 3.69#	0.827#
20–30	9.47 ± 5.66	7.38 ± 6.40	0.261	2.34 ± 5.69	-0.24 ± 4.37	0.053	3.22 ± 4.42	4.48 ± 4.82	0.296
	15.38 ± 5.44#	17.83 ± 6.78#	0.145#	-3.51 ± 5.40#	-2.31 ± 4.96#	0.342#	3.20 ± 3.99#	4.29 ± 4.51#	0.379#
30–40	15.82 ± 5.49	13.09 ± 6.72	0.127	2.79 ± 5.08	0.45 ± 4.12	0.071	5.17 ± 4.71	5.84 ± 4.76	0.588
	21.74 ± 5.65#	23.53 ± 6.72#	0.297#	-3.06 ± 6.11#	-1.61 ± 5.05#	0.249#	5.15 ± 4.56#	5.65 ± 4.56#	0.692#
40–50	23.27 ± 5.48	20.42 ± 6.87	0.110	2.97 ± 4.87	-0.56 ± 4.93	**0.011**	6.47 ± 4.62	7.12 ± 5.26	0.593
	29.19 ± 6.16#	30.86 ± 7.35#	0.363#	-2.88 ± 5.94#	-2.63 ± 4.80#	0.843#	6.44 ± 4.62#	6.93 ± 4.14#	0.667#
50–60	30.83 ± 5.96	27.60 ± 6.57	**0.046**	2.38 ± 4.43	-1.50 ± 4.70	**0.004**	8.46 ± 5.33	8.75 ± 4.94	0.830
	36.74 ± 7.14#	38.04 ± 6.67#	0.452#	-3.47 ± 6.44#	-3.57 ± 5.45#	0.939#	8.44 ± 5.23#	8.56 ± 4.44#	0.926#
60–70	37.41 ± 5.24	34.02 ± 4.56	**0.007**	1.52 ± 4.83	-1.99 ± 4.96	**0.015**	9.39 ± 5.12	9.50 ± 4.86	0.935
	43.32 ± 6.90#	44.47 ± 7.62#	0.558#	-4.32 ± 6.68#	-4.06 ± 6.75#	0.870#	9.37 ± 5.30#	9.31 ± 4.76#	0.966#

#3D tilt was normalized to a set position (i.e. full extension)

between the two groups in 3D $tilt_{axial}$ normalized to the full extension at -10° to 70° of knee flexions (all $P > 0.05$). There were no significant differences between the two groups in the 3D $tilt_{coronal}$ and 3D $tilt_{coronal}$ normalized to the full extension at -10° to 70° of knee flexions (all $P > 0.05$).

Discussion

There were three main findings in this study. Firstly, the results suggested that abnormal motion in the patellar sagittal plane might be a potential risk factor for the development of PFP. The patella elevated at knee flexions of 50° to 70° and tilted anteriorly at flexions of -10° to 10° and 50° to 70°. These findings indicated potential

sagittal patellar instability in patients with PFP. Secondly, axial and coronal patella instability may also be present in patients with PFP. The patella of patients with PFP had an axial outward tilt at flexions of -10° to 10° and 40° to 70°. It was found that when extended to 20° flexion, the patella was closer to the femoral trochlear groove in patients with PFP. Third, the angle of knee flexion affected the sagittal and axial 3D tilt of the patella. The trends in the sagittal and axial 3D tilt differed between the two groups, indicating an abnormal dynamic tilting pattern of the patella in the sagittal and axial plane in the PFP group. These findings supported our hypothesis that abnormal patella motion patterns at multiple planes might lead to the onset of PFP. Therefore, when analyzing the motion patterns of the patellofemoral joint in PFP patients, the multi- plane motion characteristics of the patella should be considered. In particular, the sagittal plane, which is easily ignored, needs to be paid attention to.

The position of the patella in relation to the trochlea significantly impacts patellofemoral stability and can contribute to potential pain [29]. Davies et al. [30] found that an elevated patellar position is an important and common anatomical factor in patients with PFP. Patella alta increases the quadriceps moment arm, leading to greater compression forces and reducing the patellofemoral contact area between 0° and 60° of flexion. These anomalies will increase the risk of cartilage degeneration and subsequent pain [31]. A biomechanical study indicated that as knee flexion exceeds 60°, there was a notable increase in patellofemoral contact force when the patella was elevated [32]. Our study found that compared to the control group, the patella was elevated in the PFP group when the knee was flexed at 50° -70°. This suggests that abnormal patellar height changes may be associated with the occurrence of PFP. Saikat Pal et al. [33] found that the patellar height in the PFP group was elevated compared to the normal control group when in an upright, weight-bearing position. However, no differences were observed near full extension in the current study, which is consistent with the findings of Nicole A. et al. [24] This demonstrates that the knee flexion angle during imaging is one of the key influencing factors in assessing the kinematics characteristics of the patellofemoral joint.

This study observed differences in sagittal plane shift at higher knee flexion angles. Focusing solely on the extended position seems to be incomplete. It is important to emphasize the assessment of patellar instability throughout the entire range of knee motion, as this may provide more value for diagnosing PFP. Several studies have measured patellofemoral joint alignment parameters at different knee flexion angles based on static magnetic resonance imaging to assess patellofemoral joint instability [34, 35]. Although static imaging can provide detailed anatomical information, they do not take into account the role of the quadriceps, which affects the kinematics and stability of the patellofemoral joint [36]. Grant et al. [37] also showed that the ability to detect patellar maltracking can be improved in a state of quadriceps activity. Therefore, more and more studies are advocating the assessment of patellar instability in a dynamic situation [22, 38, 39]. 4D-CT allows for imaging of the knee joint during active flexion and extension, providing volumetric data throughout the entire range of knee motion [40]. The quality of the image data obtained in this study also suggests that 4D-CT is an effective technique for analyzing patellofemoral joint movement patterns.

The motion of the patella relative to the femur involves translation and rotation in three directions: coronal, axial, and sagittal [41], so it is necessary to assess the patellofemoral alignment modalities based on multiple planes. In this study, it was found that compared with the control group, the patella of patients in the PFP group moved backward on the coronal plane. When the knee joint was in extension and flexion at 40° to 70°, patients in the PFP group tilted axially outward. The stability of the patellofemoral joint is maintained by both skeletal structure and muscles. The patella enters the femoral trochlear groove at 30° of flexion. However, the patella in the PFP group began to show a tendency to tilt outward when the knee was flexed to 40°. This may be due to the greater role of the peripatellar muscles at this time. Additionally, we found that patients in the PFP group exhibited a tendency to tilt the patella forward compared to normal controls. Anterior patellar tilt may result in the reduced contact area between the patella and the femoral trochlear groove, increased contact pressure on the patellofemoral joint, and leading to PFP. This is consistent with a study that have proposed theoretical models of the pathological biomechanics of PFP [15].

At present, there is no consensus on the etiology of PFP, and there is a lack of primary etiological evidence as a basis for treatment [42]. One study suggested that the occurrence of PFP may be related to patellar maltracking [15]. Our study found that patients with PFP have multiplanar patellar maltracking, especially in the easily overlooked sagittal plane. These results may help determine the etiology of PFP. The abnormal multiplanar tracking patterns observed in this study may result from medial quadriceps muscle weakness, an imbalance in the stiffness of the knee extensor tendons, or a combination of these factors. Biomechanical parameters of gait in the sagittal plane, such as knee flexion moment and angle, are associated with mechanical loading on the patellofemoral joint and progression of knee osteoarthritis [43–45]. Patients with PFP can be given functional training to enhance quadriceps strength and gait retraining to correct patellar maltracking, thereby reducing pain and alleviating dysfunction. Our research results provide

theoretical support for optimizing PFP treatment options and rehabilitation treatment.

To eliminate the effect of body size between different subjects, we normalized the 3D shift based on the TEA. Results from the 3D $shift_{sagittal}$ at knee flexions of 50° to 70° in the PFP group showed elevation of the patella. However, the 3D $shift_{sagittal}$ normalized to TEA showed that the patella was not elevated. In addition, results of 3D $shift_{coronal}$ have shown that the patella in patients with PFP was closer to the femoral trochlear groove when the knee was extended to 20° of flexion. However, the 3D $shift_{coronal}$ normalized to the TEA showed that the patella was farther away from the femoral trochlear groove in the PFP group. This seemed to be a better explanation that patellar anterior shift may lead to a decrease in the contact area between the patella and femoral trochlea, an increase in the contact pressure of the patellofemoral joint, and lead to PFP. Therefore, such standardization is important to ensure the comparability of measurements between subjects of different body sizes. To observe more or less movement of the patella within the PFP or control group, we normalized the data to the extended position. The results showed that during knee flexion, the changes in the PFP group and the control group were consistent.

A study by Aksahin et al. [46] and Chen et al. [47] found that the patella was tilted posteriorly with respect to the patellar ligament in patients with chondromalacia patellae or PFP. In this study, we quantitatively measured the spatial position of the patella relative to the sagittal plane of the femur based on the established patellofemoral coordinate system. We found that the patella was tilted forward relative to the femur. Due to the diversity of imaging methods and differences in measurement methods, it is difficult to integrate existing research results. Previous studies have mostly quantitatively assessed patellofemoral joint stability based on 2D linear parameters. The reference lines used on the 2D image do not match the reference lines measured in 3D space. This may lead to inconsistencies between the 3D and 2D analysis results. Conventional 2D measurements of the patellofemoral joint anatomical index are influenced by the selection of slices and reference lines [48]. In this study, 3D measurement was performed based on the established patellofemoral joint coordinate system, and the tracking of the patella relative to the femur was directly recorded. Compared with traditional 2D measurement, dynamic 3D measurement reflects the spatial movement of the patella and the activation of surrounding muscles and soft tissues under the functional state of the patellofemoral joint, thereby obtaining more realistic, objective, and repeatable results.

This study still has some limitations. First, muscle activation can occur during dynamic CT scanning, but the level of muscle activation during scanning is generally lower compared to the muscle strength when the patella is dislocated during exercise. Ideally, we should conduct research under weight-bearing conditions to better simulate actual exercise situations. Second, in order to maximize the sample size, we did not strictly match the sex of the subjects in the two groups. Previous studies have shown that although women are more likely to develop PFP than men, patellar tracking does not show significant sex differences [49]. Third, a comparison of 2D and 3D parameters was not performed in this study, and the differences between 2D and 3D parameters are unknown. Fourth, although the current study evaluated patellofemoral joint kinematics with the knee flexed to 70°, the movement patterns may be different as knee flexion deepens further and patellar motion becomes less restricted. Finally, the results of the 3D parameters in this study can only illustrate the phenomena present in the sample of this study, and the actual value in the pathogenesis of PFP still needs to be verified by relevant biomechanical studies.

Conclusion

PFP has multi-plane patellofemoral joint instability, which should be analyzed more comprehensively from multiple planes and multiple angles. The effectiveness and practical clinical value of tracking abnormal patella in different planes in the development of PFP requires more in-depth research.

Abbreviations

PFP	Patellofemoral pain
4D-CT	Four-dimensional computed tomography
3D	Three-dimensional
2D	Two-dimensional
KL	Kellgren-Lawrence
PRPP	Patellar ridge proxima point
PDP	Patella distal pole
PMP	Patella medial pole
PLP	Patella lateral pole
LFC	Lateral femoral condyle point
MFC	Medial femoral condyle point
RA	Roman arch
TEA	Transepicondylar axis
ANOVA	Analysis of Variance
ICCs	Intraclass correlation coefficients
CI	Confidence interval

Acknowledgements

Not applicable.

Author contributions

FR.L. conceptualized the study, reviewed the manuscript, Lead author of original trial data. F.Y. conceptualized the study, analyzed the data and reviewed the manuscript. M.Y. collected and analyzed the data, Wrote the manuscript. YR.C. carried out the statistical analysis, Wrote the manuscript. J.L. and HT.Y. engaged in the literature search, carried out the statistical analysis and provided critical revision. All authors read and approved the final manuscript. M.Y. and YR.C. contribute equally to this work. F.Y. and FR.L. are co-corresponding authors.

Funding
This research did not receive any specific grant from funding agencies in the public, commercial, or not-for-profit sector.

Data availability
No datasets were generated or analysed during the current study.

Declarations

Ethics approval and consent to participate
Institutional Review Board approval was obtained (The First Affiliated Hospital of Chongqing Medical University institutional review board, No. 2023 – 360). All individuals have individual rights that are not to be infringed, and informed consent was obtained from all individual participants included in the study.

Consent for publication
Written informed consent for publication was obtained from all participants.

Competing interests
The authors declare no competing interests.

Received: 13 November 2024 / Accepted: 14 February 2025
Published online: 24 February 2025

References

1. Barton CJ, Crossley KM. Sharing decision-making between patient and clinician: the next step in evidence-based practice for patellofemoral pain? Br J Sports Med. 2016;50(14):833–4.
2. Mølgaard C, Rathleff MS, Simonsen O. Patellofemoral pain syndrome and its association with hip, ankle, and foot function in 16- to 18-year-old high school students: a single-blind case-control study. J Am Podiatr Med Assoc. 2011;101(3):215–22.
3. Hall R, Barber Foss K, Hewett TE, Myer GD. Sport specialization's association with an increased risk of developing anterior knee pain in adolescent female athletes. J Sport Rehabil. 2015;24(1):31–5.
4. Thijs Y, De Clercq D, Roosen P, Witvrouw E. Gait-related intrinsic risk factors for patellofemoral pain in novice recreational runners. Br J Sports Med. 2008;42(6):466–71.
5. Collins NJ, Oei EHG, de Kanter JL, Vicenzino B, Crossley KM. Prevalence of Radiographic and Magnetic Resonance Imaging Features of Patellofemoral Osteoarthritis in Young and Middle-aged adults with Persistent Patellofemoral Pain. Arthritis Care Res (Hoboken). 2019;71(8):1068–73.
6. Hinman RS, Lentzos J, Vicenzino B, Crossley KM. Is patellofemoral osteoarthritis common in middle-aged people with chronic patellofemoral pain? Arthritis Care Res (Hoboken). 2014;66(8):1252–7.
7. Lanois CJ, Collins N, Neogi T, Guermazi A, Roemer FW, LaValley M, et al. Associations between anterior knee pain and 2-year patellofemoral cartilage worsening: the MOST study. Osteoarthritis Cartilage. 2024;32(1):93–7.
8. Rathleff MS, Rathleff CR, Olesen JL, Rasmussen S, Roos EM. Is knee Pain during Adolescence a self-limiting Condition? Prognosis of Patellofemoral Pain and other types of knee Pain. Am J Sports Med. 2016;44(5):1165–71.
9. Lankhorst NE, van Middelkoop M, Crossley KM, Bierma-Zeinstra SM, Oei EH, Vicenzino B, et al. Factors that predict a poor outcome 5–8 years after the diagnosis of patellofemoral pain: a multicentre observational analysis. Br J Sports Med. 2016;50(14):881–6.
10. Nunes GS, Stapait EL, Kirsten MH, de Noronha M, Santos GM. Clinical test for diagnosis of patellofemoral pain syndrome: systematic review with meta-analysis. Phys Ther Sport. 2013;14(1):54–9.
11. Boling M, Padua D, Marshall S, Guskiewicz K, Pyne S, Beutler A. Gender differences in the incidence and prevalence of patellofemoral pain syndrome. Scand J Med Sci Sports. 2010;20(5):725–30.
12. Cook C, Hegedus E, Hawkins R, Scovell F, Wyland D. Diagnostic accuracy and association to disability of clinical test findings associated with patellofemoral pain syndrome. Physiother Can. 2010;62(1):17–24.
13. Smith BE, Selfe J, Thacker D, Hendrick P, Bateman M, Moffatt F, et al. Incidence and prevalence of patellofemoral pain: a systematic review and meta-analysis. PLoS ONE. 2018;13(1):e0190892.
14. Sakai N, Luo ZP, Rand JA, An KN. The influence of weakness in the vastus medialis oblique muscle on the patellofemoral joint: an in vitro biomechanical study. Clin Biomech (Bristol). 2000;15(5):335–9.
15. Powers CM, Witvrouw E, Davis IS, Crossley KM. Evidence-based framework for a pathomechanical model of patellofemoral pain: 2017 patellofemoral pain consensus statement from the 4th international Patellofemoral Pain Research Retreat, Manchester, UK: part 3. Br J Sports Med. 2017;51(24):1713–23.
16. Farrokhi S, Keyak JH, Powers CM. Individuals with patellofemoral pain exhibit greater patellofemoral joint stress: a finite element analysis study. Osteoarthritis Cartilage. 2011;19(3):287–94.
17. Best MJ, Tanaka MJ, Demehri S, Cosgarea AJ. Accuracy and reliability of the Visual Assessment of Patellar Tracking. Am J Sports Med. 2020;48(2):370–75.
18. Watts RE, Gorbachova T, Fritz RC, Saad SS, Lutz AM, Kim J, et al. Patellar Tracking: An Old Problem with New insights. Radiographics. 2023;43(6):e220177.
19. Senavongse W, Amis AA. The effects of articular, retinacular, or muscular deficiencies on patellofemoral joint stability: a biomechanical study in vitro. J Bone Joint Surg Br. 2005;87(4):577–82.
20. Blum A, Gillet R, Rauch A, Urbaneja A, Biouichi H, Dodin G, et al. 3D reconstructions, 4D imaging and postprocessing with CT in musculoskeletal disorders: past, present and future. Diagn Interv Imaging. 2020;101(11):693–705.
21. Gondim Teixeira PA, Formery AS, Hossu G, Winninger D, Batch T, Gervaise A, et al. Evidence-based recommendations for musculoskeletal kinematic 4D-CT studies using wide area-detector scanners: a phantom study with cadaveric correlation. Eur Radiol. 2017;27(2):437–46.
22. Tanaka MJ, Elias JJ, Williams AA, Demehri S, Cosgarea AJ. Characterization of patellar maltracking using dynamic kinematic CT imaging in patients with patellar instability. Knee Surg Sports Traumatol Arthrosc. 2016;24(11):3634–41.
23. Williams AA, Elias JJ, Tanaka MJ, Thawait GK, Demehri S, Carrino JA, et al. The relationship between tibial tuberosity-trochlear groove Distance and abnormal patellar tracking in patients with unilateral patellar instability. Arthroscopy. 2016;32(1):55–61.
24. Wilson NA, Press JM, Koh JL, Hendrix RW, Zhang LQ. In vivo noninvasive evaluation of abnormal patellar tracking during squatting in patients with patellofemoral pain. J Bone Joint Surg Am. 2009;91(3):558–66.
25. Huang W, Zeng X, Man GC, Yang L, Zhang Y. Simultaneous Measurement of Patellofemoral Joint Kinematics and contact mechanics in Intact Knees: a cadaveric study. Orthop Surg. 2022;14(9):2317–29.
26. Servant C. Editorial Commentary: the best index to determine whether to Medialize the tibial tubercle in patients with patellar instability may be tibial tubercle to Trochlear groove Distance/Trochlear Width, but check the intraoperative Patellar Tracking as Well. Arthroscopy. 2022;38(4):1299–301.
27. Yamada Y, Toritsuka Y, Nakamura N, Horibe S, Sugamoto K, Yoshikawa H, et al. Correlation of 3D shift and 3D tilt of the Patella in patients with recurrent dislocation of the Patella and healthy volunteers: an in vivo analysis based on 3-Dimensional Computer models. Am J Sports Med. 2017;45(13):3111–18.
28. Yamada Y, Toritsuka Y, Nakamura N, Hiramatsu K, Mitsuoka T, Sugamoto K. Open wedge high tibial osteotomy does not decrease patellar height relative to femur: a three-dimensional computer model analysis. J Orthop Sci. 2023;28(5):1052–59.
29. Dejour DH, Mesnard G, Giovannetti de Sanctis E. Updated treatment guidelines for patellar instability: un menu à La Carte. J Exp Orthop. 2021;8(1):109.
30. Davies AP, Costa ML, Shepstone L, Glasgow MM, Donell S. The sulcus angle and malalignment of the extensor mechanism of the knee. J Bone Joint Surg Br. 2000;82(8):1162–6.
31. Heino Brechter J, Powers CM. Patellofemoral stress during walking in persons with and without patellofemoral pain. Med Sci Sports Exerc. 2002;34(10):1582–93.
32. Luyckx T, Didden K, Vandenneucker H, Labey L, Innocenti B, Bellemans J. Is there a biomechanical explanation for anterior knee pain in patients with patella alta? Influence of patellar height on patellofemoral contact force, contact area and contact pressure. J Bone Joint Surg Br. 2009;91(3):344–50.
33. Pal S, Besier TF, Beaupre GS, Fredericson M, Delp SL, Gold GE. Patellar maltracking is prevalent among patellofemoral pain subjects with patella alta: an upright, weightbearing MRI study. J Orthop Res. 2013;31(3):448–57.
34. Seitlinger G, Scheurecker G, Högler R, Labey L, Innocenti B, Hofmann S. The position of the tibia tubercle in 0°-90° flexion: comparing patients with patella dislocation to healthy volunteers. Knee Surg Sports Traumatol Arthrosc. 2014;22(10):2396–400.
35. Izadpanah K, Weitzel E, Vicari M, Hennig J, Weigel M, Südkamp NP, et al. Influence of knee flexion angle and weight bearing on the tibial tuberosity-trochlear groove (TTTG) distance for evaluation of patellofemoral alignment. Knee Surg Sports Traumatol Arthrosc. 2014;22(11):2655–61.

36. Sheehan FT, Borotikar BS, Behnam AJ, Alter KE. Alterations in in vivo knee joint kinematics following a femoral nerve branch block of the vastus medialis: implications for patellofemoral pain syndrome. Clin Biomech (Bristol). 2012;27(6):525–31.
37. Grant C, Fick CN, Welsh J, McConnell J, Sheehan FT. A word of caution for Future studies in Patellofemoral Pain: a systematic review with Meta-analysis. Am J Sports Med. 2021;49(2):538–51.
38. Draper CE, Besier TF, Santos JM, Jennings F, Fredericson M, Gold GE, et al. Using real-time MRI to quantify altered joint kinematics in subjects with patellofemoral pain and to evaluate the effects of a patellar brace or sleeve on joint motion. J Orthop Res. 2009;27(5):571–7.
39. Carlson VR, Boden BP, Sheehan FT. Patellofemoral Kinematics and Tibial Tuberosity-Trochlear groove distances in female adolescents with Patellofemoral Pain. Am J Sports Med. 2017;45(5):1102–09. [eng].
40. Kwong Y, Mel AO, Wheeler G, Troupis JM. Four-dimensional computed tomography (4DCT): a review of the current status and applications. J Med Imaging Radiat Oncol. 2015;59(5):545–54.
41. Yu Z, Yao J, Wang X, Xin X, Zhang K, Cai H, et al. Research methods and Progress of Patellofemoral Joint kinematics: a review. J Healthc Eng. 2019;2019:9159267.
42. Barton CJ, Lack S, Hemmings S, Tufail S, Morrissey D. The 'Best practice guide to Conservative Management of Patellofemoral Pain': incorporating level 1 evidence with expert clinical reasoning. Br J Sports Med. 2015;49(14):923–34.
43. Teichtahl AJ, Jackson BD, Morris ME, Wluka AE, Baker R, Davis SR, et al. Sagittal plane movement at the tibiofemoral joint influences patellofemoral joint structure in healthy adult women. Osteoarthritis Cartilage. 2006;14(4):331–6.
44. Farrokhi S, O'Connell M, Fitzgerald GK. Altered gait biomechanics and increased knee-specific impairments in patients with coexisting tibiofemoral and patellofemoral osteoarthritis. Gait Posture. 2015;41(1):81–5.
45. Teng HL, MacLeod TD, Link TM, Majumdar S, Souza RB. Higher knee flexion moment during the second half of the Stance Phase of Gait is Associated with the progression of Osteoarthritis of the Patellofemoral Joint on magnetic resonance imaging. J Orthop Sports Phys Ther. 2015;45(9):656–64.
46. Aksahin E, Aktekin CN, Kocadal O, Duran S, Gunay C, Kaya D, et al. Sagittal plane tilting deformity of the patellofemoral joint: a new concept in patients with chondromalacia patella. Knee Surg Sports Traumatol Arthrosc. 2017;25(10):3038–45.
47. Chen Y, Li J, Yang H, Lv F, Sheng B, Lv F. Differences in Patellofemoral Alignment between Static and dynamic extension positions in patients with Patellofemoral Pain. Orthop J Sports Med. 2024;12(3):23259671231225177.
48. Nelitz M, Lippacher S, Reichel H, Dornacher D. Evaluation of trochlear dysplasia using MRI: correlation between the classification system of Dejour and objective parameters of trochlear dysplasia. Knee Surg Sports Traumatol Arthrosc. 2014;22(1):120–7.
49. Fick CN, Jiménez-Silva R, Sheehan FT, Grant C. Patellofemoral kinematics in patellofemoral pain syndrome: the influence of demographic factors. J Biomech. 2022;130:110819.

Publisher's note